

Disproportionation and Metallization at Low-Spin to High-Spin Transition in Multiorbital Mott Systems

Jan Kuneš and Vlastimil Křápek¹

¹*Institute of Physics, Academy of Sciences of the Czech republic,
Cukrovarnická 10, Praha 6, 162 53, Czech Republic*

(Dated: March 1, 2022)

We study the thermally driven spin state transition in a two-orbital Hubbard model with crystal field splitting, which provides a minimal description of the physics of LaCoO₃. We employ the dynamical mean-field theory with quantum Monte-Carlo impurity solver. At intermediate temperatures we find a spin disproportionated phase characterized by checkerboard order of sites with small and large spin moments. The high temperature transition from the disproportionated to a homogeneous phase is accompanied by vanishing of the charge gap. With the increasing crystal-field splitting the temperature range of the disproportionated phase shrinks and eventually disappears completely.

PACS numbers: 71.10.Fd,75.30.Wx,71.30.+h,71.28.+d

The pressure or thermally driven spin state transitions play an important role in the physics of magnetic oxides [1]. A notorious example is LaCoO₃. Its peculiar magnetic and transport properties have attracted attention of physicists for decades, yet interpretation of its behavior remains controversial. The main characteristics of LaCoO₃ are the temperature (T) dependencies of the magnetic susceptibility and the conductivity [2, 3], which exhibit three distinct regions: (i) a low- T non-magnetic insulator, (ii) an intermediate- T paramagnetic insulator and (iii) a high- T paramagnetic bad metal. It is generally believed that the evolution from the non-magnetic to the paramagnetic state is due to thermal population of an excited state of the Co ion with spin (or spin and orbital) degeneracy. Commonly considered scenarios involve either low-spin to high-spin excitation [2, 4–6], low-spin to intermediate-spin excitation [7] or both [8, 9]. Temperature affects the electronic system also indirectly, by changing the crystal-field splitting through the lattice thermal expansion. Yet another possible piece to the puzzle are deformations of CoO₆ octahedra and their coupling to the spin states of the Co ion [2, 8]. Therefore it is rather difficult to distinguish the leading effects from the secondary ones.

In this Letter we study a minimal fermionic lattice model that exhibits the spin state transition. As purely electronic it does not include the effect of lattice thermal expansion or the magneto-elastic coupling. The model is essentially the same as the one studied by Werner and Millis [10], who used the dynamical mean-field theory [11] (DMFT) to map out its phase diagram at fixed temperature, and by Suzuki *et al.* [12], who studied its ground state as a function of doping by variational Monte-Carlo. We employ the DMFT method to study the temperature dependent properties in the vicinity of the boundary between the low-spin and high-spin phases. Unlike Ref. 10 we assume a specific lattice, which allows us to investigate the ordering tendencies. We compute [13] the one-

particle spectra and the local as well as the uniform spin susceptibility and find that, similar to the behavior of LaCoO₃, the model exhibits three distinct temperature regions. In addition to the low- T non-magnetic insulator and high- T local moment metal we find a spin disproportionated insulating phase at intermediate temperatures. In order to interpret the DMFT results we construct an effective low-energy Potts model, which allows analytic calculations.

Our starting point is a Hubbard Hamiltonian on a square lattice

$$\begin{aligned}
 H = & \sum_{i,\sigma} ((\Delta - \mu)n_{i,\sigma}^a - \mu n_{i,\sigma}^b) + \sum_{\langle ij \rangle, \sigma} (t_{aa} a_{i,\sigma}^\dagger a_{j,\sigma} + t_{bb} b_{i,\sigma}^\dagger b_{j,\sigma}) \\
 & + U \sum_i (n_{i,\uparrow}^a n_{i,\downarrow}^a + n_{i,\uparrow}^b n_{i,\downarrow}^b) + (U - 2J) \sum_{i,\sigma} n_{i,\sigma}^a n_{i,-\sigma}^b \\
 & + (U - 3J) \sum_{i,\sigma} n_{i,\sigma}^a n_{i,\sigma}^b,
 \end{aligned} \tag{1}$$

where $a_{i,\sigma}^\dagger, b_{i,\sigma}^\dagger$ ($a_{i,\sigma}, b_{i,\sigma}$) are the fermionic creation (annihilation) operators for a spin index σ and two types of orbitals for each lattice site i , and $n_{i,\sigma}^a, n_{i,\sigma}^b$ are the corresponding occupation number operators. The nearest-neighbor hoppings $t_{aa} = 0.45$ eV, $t_{bb} = 0.05$ eV and the on-site interaction parameters $U = 4$ eV and $J = 1$ eV are chosen to yield a broad a -band and a narrow b -band, mimicking the electronic structure of LaCoO₃. The crystal-field splitting is denoted with Δ . The T -dependent chemical potential μ is fixed to yield the average filling of 2 electrons per lattice site. Unlike Ref. 10 we consider only Ising terms in the on-site interaction.

The context of the present study is set by a conceptual form [14] of the $U - \Delta$ phase diagram of Ref. 10 shown in Fig. 1. The boundary of the metallic phase is given by opening of a linearly increasing charge gap (indicated by the color intensity). The line separating high-spin (HS) Mott and low-spin (LS) band insulator corresponds to

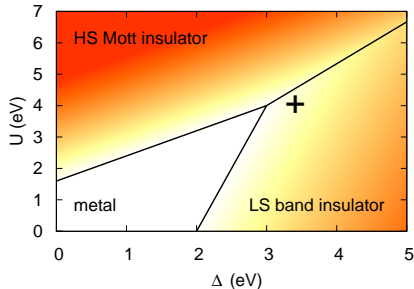


FIG. 1: (Color online) Conceptual phase diagram of the two band model for $U/J = 4$. The size of the charge gap is indicated by color intensity (white=no gap). The parameters of the present study are marked with the cross.

degeneracy of local HS and LS states. The parameter range of interest corresponding to small gap LS insulator is close to the triple point. In the following we present the results for Δ of 3.40 and 3.42 eV (marked with the cross in Fig. 1).

The DMFT equations are solved as described in Ref. 15 using the strong coupling continuous time quantum Monte-Carlo solver [16]. Guided by proposals of spin disproportionation in LaCoO_3 [2, 17] we have doubled the unit cell to allow for a spontaneous two-sublattice order (the sublattices are denoted with A and B). In the lower panel of Fig. 2 we show the occupation numbers $\bar{n}_{A,B}^a$ as a function of temperature. Below 500 K a disproportionation takes place. The local states on the A sites can be described as HS+LS statistical mixture of LS (a^0b^2) and HS (a^1b^1) configurations with short excursions to 1-electron (a^0b^1) configuration. The B sites host the LS (a^0b^2) states which experience short excursions to 3-electron (a^1b^2) configurations. The driving force of the disproportionation is a superexchange interaction mediated by these excursions, as shown in the inset of the lower panel of Fig. 2.

In the upper panel of Fig. 2 we show the local susceptibility averaged over A and B sites (the A and B contributions are shown in the inset). The local susceptibilities reflect the probability to find a given site in the HS state, while the occupancies $\bar{n}_{A,B}^a$ are to some extent affected by the charge fluctuations to 1- and 3-electrons states on A and B sites respectively. Comparison to the local susceptibility calculated in the (by constraint) homogeneous phase reveals an enhancement of the average HS abundance due to the disproportionation. We have calculated also the uniform susceptibility by adding a small Zeeman field to Eq. 1. In the disproportionated phase the uniform susceptibility coincides with the averaged local susceptibility. This is a simple consequence of the local moments on A sites being separated from each other by the B sites hosting the LS singlets. In the

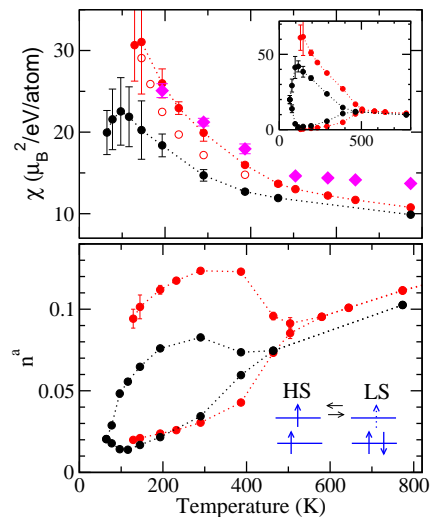


FIG. 2: (Color online) The upper panel shows the T dependence of the average local susceptibility per atom for the crystal field parameter Δ of 3.40 (red) and 3.42 (black) eV. (The site resolved contributions are shown in the inset.) The data for $\Delta = 3.40$ eV are compared to the uniform susceptibility (diamonds) and the local susceptibility obtained in the homogeneous phase (empty circles). The lower panel shows the difference $\bar{n}_A^a - \bar{n}_B^a$ of the occupancies between the A and B sites. The dotted lines are guides to the eye.

high- T homogeneous phase the uniform susceptibility is found to be enhanced over its local counterpart. This is somewhat counterintuitive since a naive expectation of an anti-ferromagnetic superexchange between the neighboring HS excitations should lead to an opposite effect. The Pauli susceptibility associated with the bad metallic state, discussed next, is an order of magnitude too small to provide an explanation. Therefore we conclude that an effective ferromagnetic coupling exists in the high- T phase.

The evolution of the one-particle spectra is shown in Fig. 3. The disproportionated phase exhibits a well-defined charge gap which starts to fill with incoherent excitations as the system approaches the transition to the homogeneous phase. To interpret this behavior we consider the definition of the charge gap in terms of the eigenenergies of the system $E_{N+1} + E_{N-1} - 2E_N$, where E_N corresponds to an eigenstate with a non-vanishing occupancy and E_{N+1} , E_{N-1} are energies of lowest states that can be reached by adding or removing an electron. At zero temperature the ground state is a product of LS (a^0b^2) configurations on each site. The lowest $N + 1$ state corresponds to a single a -electron propagating over the filled b band, while the lowest $N - 1$ state corresponds to a single b -hole. The gap is obtained as the on-site contribution reduced by half-bandwidths $U - 5J + \Delta - W_a/2 - W_b/2$.

The situation at elevated temperatures is more complicated as the initial states involve also sites in HS config-

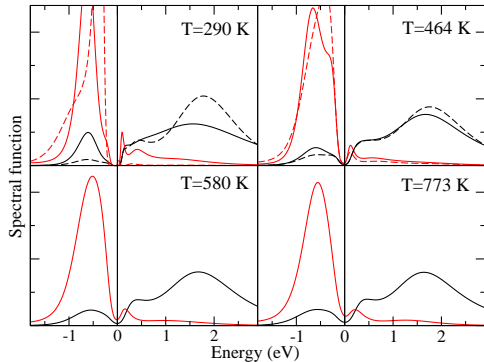


FIG. 3: (Color online) The T evolution the one-particle spectra for $\Delta = 3.40$. The spectral densities of different orbitals are resolved by color: a (black) and b (red), while the dashed lines correspond to the B sites and full lines to the A sites.

uration as well as sites with one or three electrons. The disproportionated and the homogeneous phases differ in the constraints posed on the relaxation of $N+1$ and $N-1$ excitations by the states of the neighboring sites. While in the homogeneous phase each site has neighbors which fluctuate into 1- and 3-electron states, in the disproportionated phase fluctuations are either to 1-electron states on A sites or 3-electron states on B sites. As an example we discuss the b -electron excitations on an A site from the HS initial configuration. (The LS initial configurations contribute with completely filled valence band.) In the disproportionated phase the energy of lowest $N+1$ state reached by adding b electron consists of the on-site contribution reduced by $W_a/2$ due to a electron hopping. The lowest $N-1$ state reached by b electron removal corresponds to (a^1b^1) configuration on the A site and (a^0b^1) configuration on the neighboring B site. The corresponding gap estimate is still finite $(U-2J-W_a/2)$. In the homogeneous phase the lowest $N-1$ excitation connected with b electron removal is the same as just mentioned. For $N+1$ excitations there is an additional possibility in the homogeneous phase to add b electron on a site in HS state while its neighbor is in (a^0b^1) configuration leading to the (a^0b^2) final state with (a^1b^1) on the neighboring site after a electron transfer. Considering these excitations we obtain a vanishing estimate for the charge gap.

In order to gain insight into the DMFT results we integrate out charge fluctuations in (1) to get an effective Potts model with three lowest-energy states (LS, HS \uparrow , HS \downarrow) per site

$$\tilde{H} = \xi_0 \sum_{i,\sigma} n_{i,\sigma}^{\text{HS}} + \sum_{\langle ij \rangle, \sigma} (\xi_1 n_i^{\text{LS}} n_{j,\sigma}^{\text{HS}} + \xi_2 n_{i,\sigma}^{\text{HS}} n_{j,-\sigma}^{\text{HS}}). \quad (2)$$

Here $n_{i,\sigma}^{\text{HS}}$ and n_i^{LS} are the projectors of the three states.

The coupling constants arising from lowest order virtual hopping processes read $\xi_0 = \Delta - 3J$, $\xi_1 = -\frac{t_{aa}^2}{U+J}$, and $\xi_2 = -\frac{2t_{aa}^2}{U+J}$. It should be pointed out that this model is only good for qualitative comparison to the DMFT data as the charge fluctuations are not negligible (in particular in the metallic phase). A mean-field decoupling of (2) allowing for a two sublattice order leads to the free energy per site expression

$$\begin{aligned} F(T) = & \frac{\xi_0}{2}(x_A + x_B) + 2\xi_1(x_A + x_B - 2x_Ax_B) - \xi_2x_Ax_B \\ & + \frac{T}{2}(1-x_A)\ln(1-x_A) + \frac{T}{2}(1-x_B)\ln(1-x_B) \\ & + \frac{T}{2}x_A\ln\left(\frac{x_A}{2}\right) + \frac{T}{2}x_B\ln\left(\frac{x_B}{2}\right), \end{aligned} \quad (3)$$

where $x_{A,B}$ are the mean values of $n_{\uparrow}^{\text{HS}} + n_{\downarrow}^{\text{HS}}$ on the two sublattices. The equilibrium values of $x_A - x_B$ obtained by minimization of (3) are shown in Fig. 4 together with corresponding uniform spin susceptibility. For $\xi_0 > 4\xi_1$ we find a uniform LS ground state at $T = 0$, which is followed by a transition into the disproportionated phase characterized by $x_A \neq x_B$ between temperatures T_{c1} and T_{c2} . With increasing ξ_0 the T_{c1} and T_{c2} converge and the disproportionated phase eventually disappears for large enough ξ_0 .

The disproportionated phase exhibits an enhanced susceptibility, which has two sources. First, like in the DMFT results the HS abundance is enhanced with respect to the homogeneous phase. Second, in the homogeneous phase the anti-ferromagnetic (AFM) coupling ξ_2 reduces the uniform susceptibility. Note that this is in contrast to the DMFT results.

The HS-LS model is not new. It was suggested for LaCoO₃ by Goodenough and Raccach [2] and the disproportionation was studied by Bari and Sivardi re [18]. However, traditionally the interaction between the LS and HS state was associated with the magneto-elastic coupling, namely a breathing distortion of the CoO₆ octahedra. This is quite different from the present work where the disproportionation is of purely electronic origin.

Finally, we discuss the implications of our results in the context of LaCoO₃. We show that physics of LaCoO₃ over the whole temperature range can be qualitatively described by purely electronic effects and with only one local moment state. The simplicity of the present model lends it generality, but inevitably involves approximations. First, our model involves two non-degenerate orbitals while LaCoO₃ is characterized by three-fold quasi-degenerate t_{2g} and two-fold degenerate e_g orbitals leading to different entropic contributions. Nevertheless, the main control parameters are the coupling constants, and different band degeneracies have only quantitative effect. Second, the Co-O bond-lengths change due to the nor-

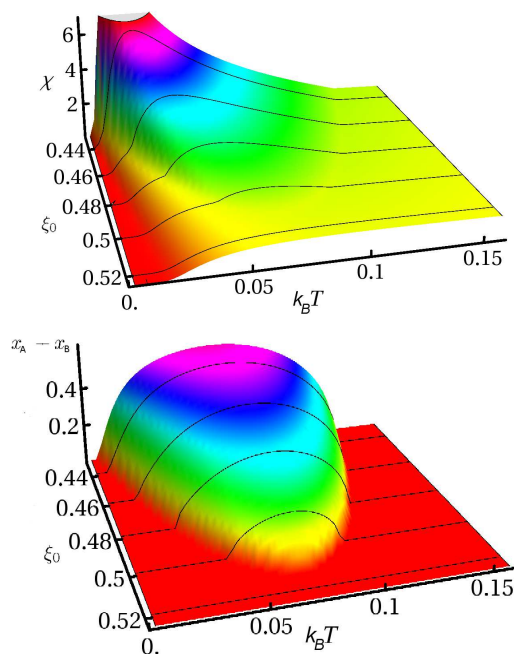


FIG. 4: (Color online) The uniform susceptibility of the Potts model as a function of temperature and the parameter ξ_0 . (upper panel) The difference of the HS populations $x_A - x_B$ as a function of temperature and ξ_0 . (lower panel)

mal and anomalous lattice thermal expansion [8]. The latter is caused by populating the HS state, well-known to weaken the metal ion–ligand bonds [19, 20]. Considering a path of decreasing $\xi_0(T)$ in Fig. 4 it is clear that the lattice response enhances the observed effects as smaller crystal field favors the disproportionation as well as the metallization. Third, no disproportionation and corresponding breathing lattice distortion was observed in recent experiments [8, 21]. It is well known that mean-field approximations overestimate ordering tendencies and that a long-range order in the mean-field solution is often indicative of short-range correlations in the system. Therefore we speculate that in LaCoO_3 dynamical HS-LS correlations take place. It is plausible that such a dynamical effect can arise from the instantaneous HS-LS interaction of electronic origin. On the other hand, magneto-elastic HS-LS interaction retardation effects due to the lattice dynamics are likely to weaken dynamical HS-LS correlation considerably. Fourth, two regions of Curie-Weiss behavior observed in experiments have been interpreted as an evidence for two different local moment states (high-spin and intermediate-spin) [9]. In our model we observe different behaviors of the uniform susceptibility in the disproportionated and in the homogeneous high T phase. The difference has three sources: (i) an enhanced abundance of the HS configurations in the disproportionated phase (over a hypothetical homogeneous phase at the same T), (ii) absence of the nearest-neighbor

anti-ferromagnetic correlations in the disproportionated phase, (iii) the metallicity of the homogeneous phase.

In conclusion, we have used numerical DMFT method to study a two-band Hubbard model with quasi-degenerate high-spin and low-spin local states. Varying temperature we have observed three different regimes: a low-spin insulator, an insulating phase with HS-LS disproportionation and enhanced Curie-Weiss susceptibility and a homogeneous metallic phase with Curie-Weiss susceptibility. We have argued that our model study captures the essential physics of LaCoO_3 and thus that the properties of LaCoO_3 can be explained with a single magnetic moment carrying state and without the effect of the lattice thermal expansion.

We thank Z. Jiráček and P. Novák for numerous discussions and critical reading of the manuscript. This work was supported by the Grant No. P204/10/0284 of the Grant Agency of the Czech Republic and by the Deutsche Forschungsgemeinschaft through FOR1346.

-
- [1] P. Gütlich and H. A. Goodwin, *Spin Crossover in Transition Metal Compounds I* (Springer-Verlag, 2004).
 - [2] P. M. Raccah and J. B. Goodenough, *Phys. Rev.* **155**, 932 (1967).
 - [3] K. Asai, O. Yokokura, N. Nishimori, H. Chou, J. M. Tranquada, G. Shirane, S. Higuchi, Y. Okajima, and K. Kohn, *Phys. Rev. B* **50**, 3025 (1994).
 - [4] R. R. Heikes, R. C. Miller, and R. Mazelsky, *Physica* **30**, 1600 (1964).
 - [5] C. S. Naiman, R. Gilmore, B. DiBartolo, A. Linz, and R. Santoro, *Journal of Applied Physics* **36**, 1044 (1965).
 - [6] A. Podlesnyak, S. Streule, J. Mesot, M. Medarde, E. Pomjakushina, K. Conder, A. Tanaka, M. W. Haverkort, and D. I. Khomskii, *Phys. Rev. Lett.* **97**, 247208 (2006).
 - [7] M. A. Korotin, S. Y. Ezhov, I. V. Solovyev, V. I. Anisimov, D. I. Khomskii, and G. A. Sawatzky, *Phys. Rev. B* **54**, 5309 (1996).
 - [8] P. G. Radaelli and S.-W. Cheong, *Phys. Rev. B* **66**, 094408 (2002).
 - [9] K. Asai, A. Yoneda, O. Yokokura, J. M. Tranquada, G. Shirane, and K. Kohn, *J. Phys. Soc. Jpn.* **67**, 290 (1998).
 - [10] P. Werner and A. J. Millis, *Phys. Rev. Lett.* **99**, 126405 (2007).
 - [11] A. Georges, G. Kotliar, W. Krauth, and M. J. Rozenberg, *Rev. Mod. Phys.* **68**, 13 (1996).
 - [12] R. Suzuki, T. Watanabe, and S. Ishihara, *Phys. Rev. B* **80**, 054410 (2009).
 - [13] A. Albuquerque, F. Alet, P. Corboz, P. Dayal, A. Feiguin, S. Fuchs, L. Gamper, E. Gull, S. Gürtler, A. Honecker, et al., *Journal of Magnetism and Magnetic Materials* **310**, 1187 (2007).
 - [14] J. Kuneš, I. Leonov, M. Kollar, K. Byczuk, V. Anisimov, and D. Vollhardt, *Eur. Phys. J. Special Topics* **180**, 5 (2009).
 - [15] J. Kuneš, V. I. Anisimov, A. V. Lukoyanov, and D. Vollhardt, *Phys. Rev. B* **75**, 165115 (2007).

- [16] P. Werner, A. Comanac, L. de' Medici, M. Troyer, and A. J. Millis, Phys. Rev. Lett. **97**, 076405 (2006).
- [17] K. Knížek, Z. Jirák, J. Hejtmánek, P. Novák, and W. Ku, Phys. Rev. B **79**, 014430 (2009).
- [18] R. A. Bari and J. Sivardière, Phys. Rev. B **5**, 4466 (1972).
- [19] J. Badro, G. Fiquet, V. V. Struzhkin, M. Somayazulu, H.-k. Mao, G. Shen, and T. Le Bihan, Phys. Rev. Lett. **89**, 205504 (2002).
- [20] J. Kuneš, D. M. Korotin, M. A. Korotin, V. I. Anisimov, and P. Werner, Phys. Rev. Lett. **102**, 146402 (2009).
- [21] G. Maris, Y. Ren, V. Volotchaev, C. Zobel, T. Lorenz, and T. T. M. Palstra, Phys. Rev. B **67**, 224423 (2003).